Muscle and Heart Function Restoration in a Limb Girdle Muscular Dystrophy 2I (LGMD2I) Mouse Model by Systemic *FKRP* Gene Delivery

Chunping Qiao[1], Chi-Hsien Wang[1,2], Chunxia Zhao[1,3], Peijuan Lu[4], Hiroyuki Awano[4], Bin Xiao[1], Jianbin Li[1], Zhenhua Yuan[1], Yi Dai[5], Carrie Bette Martin[1], Juan Li[1], Qilong Lu[4] and Xiao Xiao[1]

[1]Division of Molecular Pharmaceutics, Eshelman School of Pharmacy, University of North Carolina, Chapel Hill, North Carolina, USA; [2]Graduate Institute of Injury Prevention and Control, College of Public Health and Nutrition, Taipei Medical University, Taipei, Taiwan; [3]Cardiovascular Division of Internal Medicine, Tongji Hospital, Tongji Medical college, Huazhong University of Science and Technology, Wuhan, PR China; [4]McColl-Lockwood Laboratory for Muscular Dystrophy Research, Neuromuscular/ALS Center, Carolinas Medical Center, Charlotte, North Carolina, USA; [5]Department of Neurology, Peking Union Medical College Hospital, Peking Union Medical College and Chinese Academy of Medical Sciences, Beijing, China

Mutations in fukutin-related protein (*FKRP*) gene cause a wide spectrum of disease phenotypes including the mild limb-girdle muscular dystrophy 2I (LGMD2I), the severe Walker-Warburg syndrome, and muscle-eye-brain disease. FKRP deficiency results in α-dystroglycan (α-DG) hypoglycosylation in the muscle and heart, which is a biochemical hallmark of dystroglycanopathies. To study gene replacement therapy, we generated and characterized a new mouse model of LGMD2I harboring the human mutation leucine 276 to isoleucine (L276I) in the mouse alleles. The homozygous knock-in mice (*L276I*^{KI}) mimic the classic late onset phenotype of LGMD2I in both skeletal and cardiac muscles. Systemic delivery of human *FKRP* gene by AAV9 vector in the *L276I*^{KI} mice, at either neonatal age or at the age of 9 months, rendered body wide FKRP expression and restored glycosylation of α-DG in both skeletal and cardiac muscles. *FKRP* gene therapy ameliorated dystrophic pathology and cardiomyopathy such as muscle degeneration, fibrosis, and myofiber membrane leakage, resulting in restoration of muscle and heart contractile functions. Thus, these results demonstrated that the treatment based on *FKRP* gene replacement was effective.

Received 22 January 2014; accepted 16 July 2014; advance online publication 19 August 2014. doi:10.1038/mt.2014.141

INTRODUCTION

Muscular dystrophies (MDs) are a class of hereditary, degenerative disorders of striated muscles. MDs are caused by defects in genes that encode a diverse group of proteins.[1] Among them, a subset of MDs shares the same biochemical feature of reduced glycosylation of α-dystroglycan and diminished laminin binding activity, collectively termed dystroglycanopathies.[2] They are a heterogeneous group of autosomal recessive diseases with a wide spectrum of clinical severities.[3,4]

Dystroglycan (DG) consists of a heavily glycosylated extracellular α subunit (α-DG) and a transmembrane β subunit (β-DG). α-DG and β-DG are encoded by a single gene and post-translationally cleaved to generate the two subunits.[5] α-DG is a cell surface receptor for several extracellular matrix proteins such as laminin, agrin, and perlecan in muscle,[6] and neurexin in brain.[7] The trans-membrane β-DG anchors α-DG at the cell surface and binds intracellularly to dystrophin, which in turn binds to the actin cytoskeleton. Thus, DG functions as a molecular anchor, connecting the extracellular matrix with the cytoskeleton across the plasma membrane in skeletal muscle.[8] Deficiencies of proteins and enzymes involved in the pathways of α-DG post-translational modification, *e.g.*, glycosylation, are chiefly responsible for dystroglycanopathies. The dystroglycanopathies account for the second most common group of MDs, only less frequent than Duchenne muscular dystrophy (DMD).[9] Currently, more than six proteins have been identified in DG glycosylation pathway.[10–15] Specifically, protein O-mannosyltransferase 1 (POMT1), POMT2, and protein O-linked mannose N-acetylglucosaminyltransferase 1 (POMGnT1) are shown to initiate the first two steps of the O-mannosylation pathway, a unique type of O-linked glycosylation in α-DG.[16] Fukutin-related protein (FKRP) and LARGE (like-acetylglucosaminyltransferase) are involved in phosphorylation of O-linked mannose in α-DG, which is required for laminin binding.[5,17]

Mutations in the *FKRP* gene cause a wide spectrum of disease severity in muscular dystrophies. There is a general genotype–phenotype correlation in patients, despite the fact that hypoglycosylation of α-DG can be variable in FKRP associated dystroglycanopathy.[18] The milder, most common form is limb girdle muscular dystrophy 2I (LGMD2I), characterized by childhood or adult onset with a relatively benign disease course.[4] Individuals with LGMD2I are mostly homozygous for the Leu276Ile (nucleotide C826A) mutation of FKRP and show a variable but apparent reduction in α-DG immunolabeling.[18] LGMD patients with

The first two authors contributed equally to this work.

Correspondence: *Xiao Xiao, Division of Molecular Pharmaceutics, Eshelman School of Pharmacy, University of North Carolina at Chapel Hill, Chapel Hill, North Carolina, USA. E-mail: xxiao@email.unc.edu or Qilong Lu, McColl-Lockwood Laboratory for Muscular Dystrophy Research, Neuromuscular/ALS Center, Carolinas Medical Center, Charlotte, North Carolina, USA. E-mail: qi.lu@carolinashealthcare.org*

Duchenne-like severity typically have a moderate reduction in α-DG and contain compound heterozygous mutations, including the common C826A FKRP mutation and other missense or nonsense mutations.[18,19] The more severe form is the congenital muscular dystrophy type 1C (MDC1C) characterized by early onset, inability to walk, and highly elevated serum creatine kinase (CK) levels.[4] The MDC1C is a compound heterozygote between a nonsense and a missense mutation or two missense mutations.[18] The most severe forms of FKRP deficiency containing missense mutations are clinically similar to Walker-Warburg syndrome (mutation in POMT1 gene) or muscle-eye-brain disease (mutation in POMGnT1 gene), which has striking structural brain and eye defects.[20] Until recently, the lack of viable animal models has impeded research in pathogenesis and therapy. Deletion of the mouse *FKRP* gene or homozygous nonsense mutations are embryonic lethal.[21] To circumvent embryonic lethality, we previously utilized gene delivery of RNA interference technology to knock down FKRP expression, via postnatal gene delivery, creating a FKRP deficient animal model.[22] More recently, the FKRP P448L mutation knock-in animal model was generated, which resembles clinically severe MDC1C phenotypes with brain and eye involvement.[21,23]

In the current study, a mild LGMD2I animal model is generated by knocking in the common human L276I mutation, producing homozygous mice (*L276I*^{KI}) that carry this mutation. The mouse model has been extensively characterized for their phenotypes, which are found to closely recapitulate resemble the clinical pathology and phenotypes of the LGMD2I patients. Using the *L276I*^{KI} mice, we have tested adeno-associated virus (AAV)-mediated gene therapy for the treatment of LGMD2I. AAV vectors are highly efficient in transducing skeletal and cardiac muscle cells by *in vivo* gene delivery.[24,25] The vectors have been broadly used to study other types of muscular dystrophies, such as DMD[25–27] and laminin-α2 deficient congenital muscular dystrophy.[28] Here, we have used AAV9 vector to systemically deliver the *FKRP* gene into the neonatal and adult *L276I*^{KI} mice for long-term gene expression and therapeutic benefits. We found that overexpression of FKRP in both skeletal and cardiac muscle effectively restored the biochemical deficiency and normalized glycosylation of α-DG. Body wide *FKRP* gene expression showed no discernable toxicity, but prevented the development of dystrophic pathology in mice treated neonatally, and effectively ameliorated the pathology in mice treated at the adult age. More importantly, overexpression of FKRP resulted in contractile function recovery of skeletal muscles as well as cardiac muscles. Therefore, due to the lack of any effective treatment for FKRP deficient patients, the new mouse model and *FKRP* gene transfer study will facilitate our understanding of LGMD2I molecular pathogenesis as well as therapeutic developments.[21,22]

RESULTS

FKRP *L276I*^{KI} knock-in mice show both muscular dystrophy and cardiomyopathy

The LGMD2I mouse model was generated by knocking in the human mutation (nucleotide C826 to A) into the coding sequence of the mouse *FKRP* gene, resulting in amino acid replacement L276I.[21,22] The founder mice were bred to produce homozygous FKRP knock-in mice with hybrid *129/C57BL6* background, termed hybrid *L276I*^{KI} line. Additionally, the hybrid line was further back-crossed with the syngeneic *C57/BL6* mice for more than 10 generations to produce a genetically homogeneous line, termed *B6 L276I*^{KI}. The growth rate and life span of the homozygous mice were indistinguishable from their heterozygous littermates. Both hybrid and *B6 L276I*^{KI} homozygous mice were bred normally.

Both lines of homozygous *L276I*^{KI} mice displayed late onset of mild muscular dystrophic pathology. Muscle histology between heterozygous and homozygous mice was minimal at 3 months of age (**Figure 1a**). At 6 months of age, the centrally located nuclei (CN) in myofibers started to increase in the homozygous group (homo 9.4 ± 1.8% versus hetero 1.4 ± 0.6% in quadriceps, rectus femoris, muscle), ultimately reaching ~30% central nucleation in mice older than 9 months (**Figure 1b**). Compared to the severe phenotype of the FKRP P448L^{KI} model, the muscle pathology, such as fibrosis and cellular infiltration, in FKRP *L276I*^{KI} mice were often focal and not uniform in the same muscle groups. However, the degree of myofiber central nucleation and the overall interstitial fibrosis increased consistently with age.

The diaphragm of homozygous *L276I*^{KI} mice was the muscle most severely affected, as shown by pronounced membrane leakage and fibrosis, especially in the older mice (**Figure 1c**). These results are similar to that of the mdx mice of DMD model.[29] Evans blue dye was injected into 18-month-old heterozygous and homozygous mice. Evans blue is a widely used vital red fluorescent dye that is taken up by the cells with leaky cell membrane.[25] We found that the diaphragm was the major muscle that took up the dye (**Figure 1c**). Other muscles including tibialis, gastrocnemius, quadriceps, and heart had limited dye uptake as shown by increased intensity of interstitial red fluorescence (**Supplementary Figure S1**; **Figure 1c**). Additionally, we observed significant increase in fibrosis of the diaphragm, which was revealed by Sirius red/fast green staining (**Figure 1c**). A Sirius red/fast green dye staining technique, which binds selectively to collagen and non-collagen protein, respectively, is a commonly used assay to display and quantify the amount of collagen deposition occurring in the tissues. Quantitative collagen content (an indicator of the extent of fibrosis) analysis showed an increase in the diaphragm of the homozygous versus heterozygous mice (2.4 ± 0.6% versus 1.3 ± 0.2%; $n = 5$, $P < 0.05$) (**Figure 1d**). Similarly, heart tissue fibrosis also increased in the homozygous B6 *L276I*^{KI} mice (**Figure 1c**), signifying the presence of cardiomyopathy.

Another hallmark of dystrophic pathology in homozygous *L276I*^{KI} mice is elevated serum CK levels, which indicate muscle damage.[30] While the average serum CK levels in wild-type and heterozygous FKRP *L276I*^{KI} mice were below 300 units/l, all homozygous *B6 L276I*^{KI} mice (with *C57/BL6* background) had CK levels greater than 1,000 units/l (**Figure 1e**). Moreover, a trend emerged as the serum CK levels increased with age (**Figure 1e**), which was consistent with the histopathology observations (**Figure 1a**).

The homozygous *L276I*^{KI} mice had impaired muscle functions, such as shorter treadmill running distance and lower *in vitro* isometric force production. The running distance of the 9-month-old hybrid background heterozygous mice was 697 ± 97 meters, while the running distance of the age- and sex-matched homozygous *L276I*^{KI} litter mates was only 353 ± 172 meters (n was 5 in

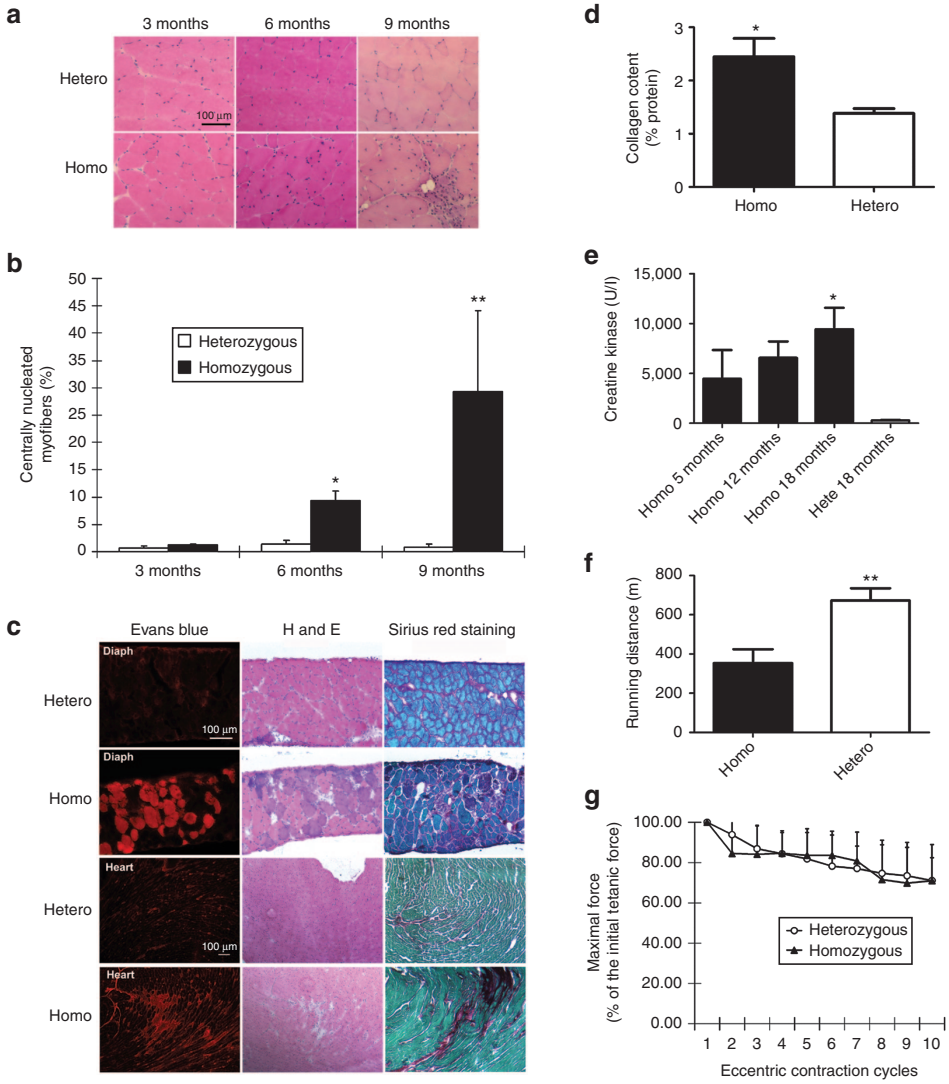

Figure 1 Characterization of homozygous FKRP *L276I*^{KI} mice. (**a**) Muscle pathology corresponding to age was displayed for both heterozygous and *B6 L276I*^{KI} homozygous mice. Cryo-thin-sections of the quadriceps muscle from different ages were analyzed with H&E staining. Large amount of centrally nucleated myofibers were observed in the quadriceps of both the 6- and 9-month-old *B6 L276I*^{KI} homozygous mice compared to the heterozygous mice. (**b**) Quantitation of centrally nucleated myofibers in homozygous versus heterozygous mice at different ages ($n = 8$; $^{*}P < 0.05$; $^{**}P < 0.001$). (**c**) Muscle leakage and fibrosis progression seen in 18 months old homozygous FKRP L276I mice. The diaphragm of homozygous FKRP *L276I*^{KI} mice (18-month-old) displayed the most dramatic dystrophic pathology as revealed by the Evans blue dye leakage, mononuclear cell infiltration (H&E staining), and fibrosis infiltration (collagen staining). Sirius red was used to stain collagen (red), and Fast green was utilized for myofiber staining (green). (**d**) Quantification of collagen content in the diaphragm muscle shown in Figure 1c. The collagen content was expressed as a percentage of the collagen (Sirius red staining) versus the noncollagen protein (fast green staining). Statistics were calculated by an unpaired *t*-test with Welch's correction ($^{*}P < 0.05$; $n = 4$). (**e**) The serum creatine kinase level was increased in homozygous mice. All homozygous *B6 L276I*^{KI} mice had CK levels greater than 1,000 units/l, and revealed a trend that the serum CK levels increase with age ($^{*}P < 0.05$ with one-way analysis of variance (ANOVA); $n = 4$–9). (**f**) The treadmill running experiment indicated homozygous mice ran shorter distance than heterozygous control ($^{**}P = 0.01$ with one-way ANOVA; $n = 5$–9). (**g**) The *in vitro* eccentric contraction force measurement. There was no difference in force production after 10 cycles of eccentric contraction challenge in the TA muscles of the homozygous mice versus heterozygous mice ($n = 6$, $P > 0.05$).

the first group and 9 in the second group, $P < 0.01$) (Figure 1f). The *in vitro* contraction measurement of the TA muscles showed a decrease in the specific isometric tetanic force of the 13-month-old hybrid homozygous *L276I*^{KI} mice compared to their heterozygous littermates (23.5 ± 2.5 versus 32.5 ± 4.5 N/cm^2, $P < 0.05$, $n = 5$) (**Supplementary Figure S2**). Unlike the dystrophin-deficient *mdx* mice,[31] the *L276I*^{KI} mice did not show a significant difference from its control heterozygous group during the 10-cycle eccentric contraction assay (lengthening activation) (Figure 1g), again suggesting mild dystrophic phenotypes. The liver and kidney functions of the homozygous mice had no abnormalities as shown by blood urea nitrogen (BUN) and serum alanine transaminase (ALT) levels (**Supplementary Figure S3**).

Systemic *FKRP* gene transfer restored glycosylation of α-dystroglycan

Our next step was to investigate the therapeutic intervention by systemic gene transfer of FKRP. Mouse codon-optimized *FKRP* gene and the ubiquitous CB promoter (CMV enhancer/chicken β-actin promoter) were used for strong and sustained transgene

expression.[32] Myc tag was fused to the C-terminus of the FKRP coding sequence to facilitate detection. The optimized *FKRP* gene was packaged into AAV9 vector which would efficiently cross the blood vessel barrier and transduce whole-body muscle cells after systemic delivery.[32]

First, we delivered the AAV9-CB-FKRP vector into neonatal mice to see whether or not overexpression of FKRP can prevent muscular dystrophic pathology in early age. AAV9-CB-FKRP-myc (1×10^{11} vector genomes (vg)/mouse) was injected intraperitoneally into 3-day-old homozygous *L276I*^{KI} mice (with hybrid background). At different time points (1 month and 9 months) after vector delivery, some of the mice (three from each group) were sacrificed for examination of transgene expression and evaluation of pathology improvement. Immunofluorescent (IF) staining against FKRP in cryo-thin-section of muscle tissue displayed strong transgene expression in all of the major muscle tissues examined (**Figure 2a**). FKRP expression appeared as punctate dots in the cytoplasmic compartment of the myofibers (**Figure 2a**), which was previously shown in the Golgi and endoplasmic reticulum (ER).[23] Also, FKRP expression in skeletal muscles was confirmed by western blot (**Figure 2b**) and anti-myc staining (**Supplementary Figure S4**).

Similar to other dystroglycanopathy animal models,[2,21] hypoglycosylation of α-DG is a feature of homozygous *L276I*^{KI} mice. To examine if overexpression of FKRP in the skeletal muscle of homozygous *L276I*^{KI} mice would restore the glycosylation of α-DG, we performed immunofluorescent staining and western blot with the widely used monoclonal antibody IIH6. IIH6 only recognizes the functional glycan epitopes of α-DG.[2] The homozygous *L276I*^{KI} skeletal muscle displayed weak or background levels of glycosylated α-DG by IF staining (**Figure 2c**). The weak glycosylation signal of α-DG was also revealed by western blot, indicating hypoglycosylation of α-DG in the skeletal muscle of the homozygous *L276I*^{KI} mice (**Figure 2b**). In contrast, the AAV-CB-FKRP-myc treated homozygous muscle displayed strong immunofluorescent signal after IIH6 antibody staining. The glycosylation of α-DG was effectively restored even 12 months after vector delivery (**Figure 2c**), making it indistinguishable from the heterozygous controls. These results demonstrated that overexpression of FKRP in skeletal muscle via AAV vector delivery fully restored the glycosylation of the α-DG in the LGMD2I mouse model.

Systemic *FKRP* gene transfer effectively ameliorates muscle pathology

We found that overexpression of FKRP in the homozygous *L276I*^{KI} mice (treated at the neonatal age) was able to normalize muscle pathology, as shown by H&E staining (**Figure 2d**). The AAV9-CB-FKRP-myc treatment of the*L276I*^{KI} mice fully prevented the formation of centrally located nuclei in the myofibers and the mononuclear cell infiltration in the muscles (**Figure 2d**). As expected, the treated mice's serum CK levels returned to normal

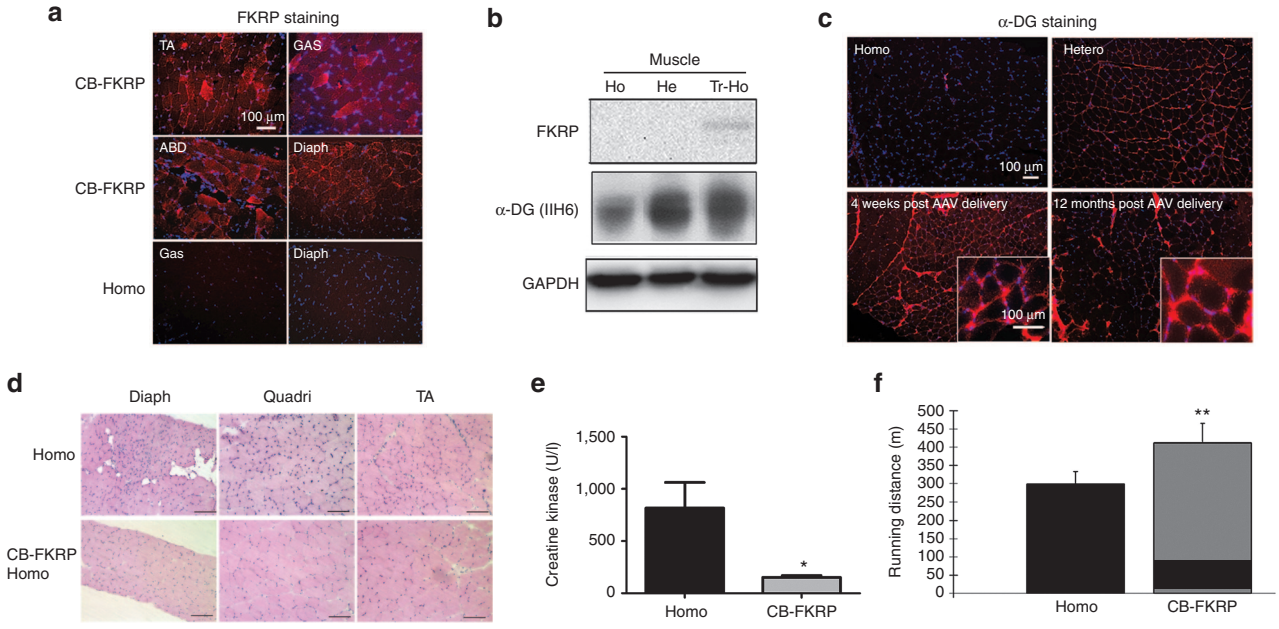

Figure 2 Improvement of muscle pathology and function after delivery of AAV9-CB-fukutin-related protein (FKRP)-myc vector in neonates. The AAV9-CB-FKRP-myc vector (1×10^{11} vg/pup) was delivered into 3-day-old homozygous pups. (**a**) Overexpression of FKRP on AAV-treated muscle. The mice (three per group) were sacrificed 1 month after adeno-associated virus (AAV) treatment, and immunofluorescent staining against FKRP was performed on the indicated tissues. ABD, abdominal muscle; Diaph, diaphragm muscle; GAS, gastrocnemius muscle; TA, tibialis muscle. (**b**) Western blot analysis of FKRP expression and glycosylated α-DG expression in quadriceps muscles from indicated mice. A total protein of 15 μg was loaded in each lane. Glyceraldehyde 3-phosphate dehydrogenase (GAPDH) was the loading control here. (**c**) Hypoglycosylation of α-DG in quadriceps muscles from homozygous FKRP *L276I*^{KI} mice and the restoration of α-DG glycosylation by AAV vector treatment. The insets were large magnification (×40) of the same area (rectus femoris quadriceps muscle) (**d**) Muscle pathology improvement revealed by H&E staining. The mice were sacrificed 9 months after treatment for pathology examination. (**e**) The serum creatine kinase levels were significantly decreased after AAV treatment. (*$P < 0.05$; $n = 5$ for homo group, and $n = 9$ for AAV9-CB-FKRP-myc treatment group). (**f**) Delivery of AAV9-CB-FKRP vector in neonatal mice (*C57/BL6* background) also improved muscle function when evaluated by the treadmill running test (**$P < 0.01$, $n = 4$–8).

(151 ± 57 units/l) in comparison to their untreated counterparts (816 ± 546 units/l, $P < 0.05$, $n = 5–9$) (**Figure 2e**). Furthermore, the muscle function improved after gene therapy in the hybrid homozygous *L276I*^{KI} mice. Treadmill tests showed that the treated homozygous mice ran much further distances (412.0 ± 53.7 meters) than their untreated counterparts (299.8 ± 33.7 meters, $P < 0.001$, $n = 4–8$).

Considering *L276I*^{KI} mice manifested delayed disease onset, we also performed gene therapy in adult homozygous mice, in order to examine whether therapeutic effects could be observed after the dystrophic pathology already appeared. The AAV9-CB-FKRP-myc vectors were delivered into 9-month-old homozygous *L276I*^{KI} mice (which corresponds to a 25-year-old human with similar symptoms) at a dosage of 6×10^{13} vg/kg via tail vein injection. Three months after vector delivery, three mice from each group were sacrificed and their tissues were utilized for pathology analysis. As anticipated, the treatment of these older mice was also able to efficiently restore the muscle morphology, shown by the H&E staining (**Figure 3a**). The centrally nucleated myofibers were significantly decreased in the treated homozygous mice (2.98 ± 0.82%) as compared to their untreated homozygous counterparts (13.89 ± 4.73%, $P < 0.001$, $n = 3$) (**Figure 3c**). The vector treatment ameliorated fibrosis infiltration as revealed by Masson's trichrome staining (**Figure 3b**). Quantitative data of collagen content failed to show statistical significance ($P > 0.05$, $n = 5$), but did indicate there was a decreasing fibrosis trend (**Figure 3d**). The treadmill running experiment demonstrated muscle function improvement by the treatment (**Figure 3e**). The treated homozygous mice ran much longer distance than the untreated littermates (697 ± 97 m versus 353 ± 172 m), and the running distance was comparable to the heterozygous controls (673 ± 108 m, $P < 0.01$, $n = 5–9$). These results indicated that delivering AAV9

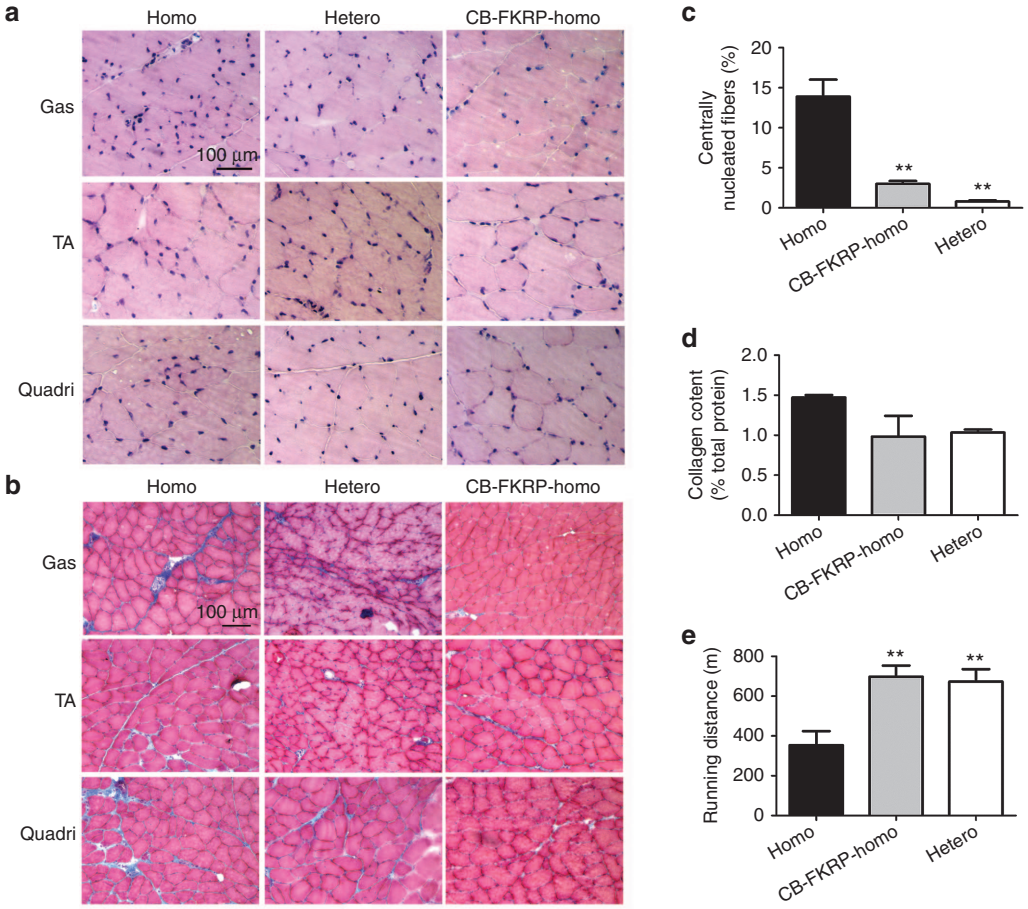

Figure 3 Delivery of AAV vector encoding fukutin-related protein (FKRP) in adult homozygous mice ameliorated dystrophic pathology and improved fibrosis infiltration. The AAV9-CB-FKRP vector was delivered into 9-month-old homozygous mice (hybrid background), and the mice were sacrificed 3 months after treatment. (**a**) H&E staining indicated that the skeletal muscle pathology was ameliorated after adeno-associated virus (AAV) treatment. Gas, gastrocnemius muscle; TA, tibialis muscle; Quadri, quadriceps (rectus femoris) muscle. (**b**) Masson's trichrome staining revealed a fibrosis infiltration reduction by the delivery of AAV vector encoding FKRP. (**c**) Quantification of centrally nucleated myofibers. All of the gastrocnemius muscle fibers (a minimum of 267 muscle fibers) were counted on each photo (objective ×10) of H&E staining, and at least three photos were included for each mouse. The percentile of centrally nucleated fibers was defined as the percentage of centrally nucleated fibers versus the total counted myofibers. The one-way analysis of variance (ANOVA) test was utilized for statistical analysis (**$P = 0.0002$; three animals were used for each group). (**d**) Quantification of collagen content in Gastrocnemius muscle. This analysis failed to show statistical significance ($P = 0.08$, $n = 5$), but did indicate there was a decreasing fibrosis trend. (**e**) Motor function recovery by AAV9-CB-FKRP treatment in older homozygous mice. The vector was delivered into 9-month-old male homozygous mice (hybrid background), and the treadmill test was performed 4 months after treatment (**$P < 0.01$ with one-way ANOVA; $n = 5$ for CB-FKRP homo and hetero groups, and $n = 9$ for homo group).

vector encoding *FKRP* gene could be therapeutic even in older homozygous mice that already displayed dystrophic pathology.

Prevention of cardiomyopathy and improvement of heart contractile capacity

It has been reported that LGMD2I patients often develop cardiomyopathy.[33] In homozygous FKRP *L276I*^{KI} mice, focal and scattered fibrosis was also observed in the cardiac muscle (**Figure 1c**). Therefore, we examined if overexpression of FKRP in the heart could improve cardiomyopathy. To achieve robust and persistent cardiac expression, we utilized an improved cardiac- and skeletal-muscle specific synthetic promoter,[34,35] in addition to the ubiquitous CB promoter. The muscle-specific promoter contained a synthetic muscle promoter[35] and an 100 bp fragment downstream of the +1 site in the chicken skeletal α-actin promoter, which was designated as syn100. The AAV9-syn100-FKRP and AAV9-CB-FKRP vectors were delivered into the neonatal homozygous *L276I*^{KI} mice (3 days old). The untreated littermates were used as the control. Seven months after vector delivery, the mice were subjected to echocardiography analysis and subsequently *FKRP* gene expression analysis. AAV9-CB-FKRP and AAV9-syn100-FKRP vector rendered strong FKRP expression in both cardiac and skeletal muscle as evidence by the IF staining (**Figure 4a**) and the western blot (**Figure 4b**). Similar to the expression pattern seen in skeletal muscle, the expression of FKRP in the heart muscle cytoplasm appeared as punctate dots, and the wild-type FKRP in heterozygous and homozygous mice could not be detected by the anti-FKRP antibody (**Figure 4a**). As expected, overexpression of FKRP by AAV9-syn100-FKRP and AAV9-CB-FKRP in homozygous mice heart restored the glycosylation of α-DG.

Finally, we investigated if gene therapy could improve cardiac function. Similar to the *mdx* mice, the FKRP *L276I*^{KI} mice displayed a mild cardiac function deficit, which is not readily detectable by regular echocardiography.[36] Therefore, we opted to evaluate the cardiac function by echocardiography (Echo) with a dobutamine challenge. Dobutamine is a sympathomimetic drug that stimulates ß1-adrenergic receptors in the heart, resulting in an increase in heart rate, contractility and demand for myocardial oxygen.[37] Clinically, the dobutamine stress test provides a more revealing diagnostic and prognostic examination for cardiomyopathy patients.[37] Echocardiography was performed before and 2 minutes after dobutamine administration on the 7-month-old homozygous, heterozygous, AAV9-syn100-FKRP-treated, and AAV9-CB-FKRP-treated homozygous mice.[38] Before dobutamine stimulation, no significant difference of cardiac systolic function was found among the four groups of mice as determined

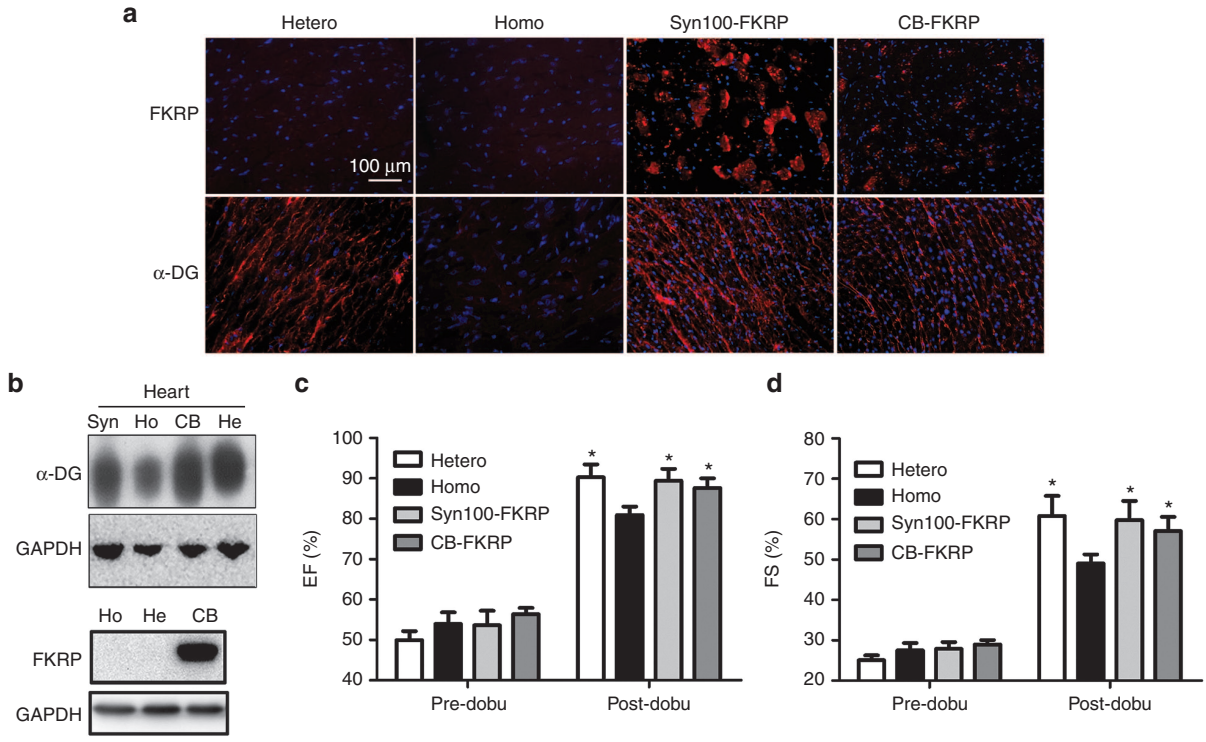

Figure 4 Restoration of α-DG glycosylation and improvement of cardiac contractile capacity by delivery of adeno-associated virus (AAV)9 encoding fukutin-related protein (*FKRP*) gene. The AAV9-syn100-FKRP and AAV9-CB-FKRP vectors (3×10^{11} vg/pup) were delivered into the neonatal mice, and age matched heterozygous and homozygous mice were used as controls. Gene expression and heart function examinations were performed 7 months after vector delivery. (**a**) Overexpression of FKRP via AAV vector, driven by muscle-specific syn100 promoter or ubiquitous CB promoter, all restored the glycosylation of α-DG in the homozygous FKRP *L276I*^{KI} mice shown by the IF staining. (**b**) The western blot further indicated that overexpression of FKRP in homozygous mice completely restored the glycosylation of α-DG. For the western blot of FKRP expression, homozygous mice were treated by AAV9-CB-FKRP vector. (**c**) The dobutamine stress Echo indicated improvement in ejection fraction (EF) for both syn100-FKRP and CB-FKRP treated groups after dobutamine stimulation. (**d**) The dobutamine stress Echo displayed enhanced cardiac contractile function in fractional shortening (FS) for both syn100-FKRP- and CB-FKRP-treated groups after dobutamine stimulation. (*$P < 0.05$, $n = 3$ for treated group, and $n = 8$ for hetero and homo groups for both **c** and **d**).

by ejection fraction (EF) and fractional shortening (FS) (**Figure 4c,d**). EF and FS are the most commonly used indexes of left ventricle contractile function. EF represents the volumetric fraction of blood pumped out of the left and right ventricle with each heartbeat, while FS measures the change in the diameter of the left ventricle between the contracted and relaxed cycles. After dobutamine stimulation, however, the EF (89.4 ± 5.1% for syn100 promoter, 87.6 ± 5.3% for CB promoter) and FS (59.75 ± 6.0% for syn100 promoter, 57.09 ± 7% for CB promoter) of the AAV-treated homozygous mice were significantly higher than the untreated homozygous mice (80.9 ± 5.1% for EF, 49.0 ± 4.9% for FS, n = 3–8, $P < 0.05$), and similar to the heterozygous control littermates (90.2 ± 5.5% for EF, 60.8 ± 8.2%) (**Figure 4c,d**). These results demonstrated that the heart of the homozygous FKRP *L276I*^{KI} mice indeed have compromised contractile capacity, and that overexpression of FKRP can completely restore original heart function.

DISCUSSION

Dystroglycanopathies have recently been recognized as the most common form of muscular dystrophies second to Duchenne muscular dystrophy. FKRP-related dystroglycanopathies are associated with a wide range of muscular dystrophies from the most common, mild form of LGMD2I with adult onset to the rare but severe Walker-Warburg syndrome or muscle eye-brain disease with brain and eye involvement.[3,18,20] Chan *et al.* [21] created a human *FKRP* mutation P448L knock-in mouse model *P448L*^{KI}, which represents the severe congenital muscular dystrophies with early onset and with brain and eye involvement. Here, we described the FKRP *L276I*^{KI} model with late onset and mild muscular dystrophic pathology reminiscent of the LGMD2I patients. The FKRP *L276I*^{KI} model mimicked the LGMD2I pathology in nearly all aspects, including the major histopathology as well as the biochemical deficiencies. Systemic gene delivery of FKRP in either neonatal mice or adult mice was able to achieve body wide *FKRP* gene expression and restoration of the α-dystroglycan glycosylation. Biochemical correction also resulted in histopathological correction for the homozygous FKRP *L276I*^{KI} mice. Furthermore, both skeletal muscle and cardiac muscle functions were recovered as shown by the treadmill running distance and the echocardiography results. Overexpression of FKRP did not reveal any discernable toxicity, suggesting gene therapy with *FKRP* gene replacement is a safe approach. Therefore, FKRP *L276I*^{KI} represents a useful model that can be used to study the mechanisms of pathogenesis as well as new therapies in the most common form of LGMD.

The disease phenotype of the homozygous B6 FKRP *L276I*^{KI} only slightly differed from that of the homozygous hybrid FKRP *L276I*^{KI}. Only the serum CK level of homozygous B6 FKRP *L276I*^{KI} was higher (**Figure 1e**) than the hybrid FKRP *L276I*^{KI} (**Figure 2e**); therefore, minimal strain variations was indicated in this study. Furthermore, the mild FKRP *L276I*^{KI} model of LGMD2I can also be converted into a more severe animal model by creating a compound heterozygous mutation line through breeding with a severe FKRP mouse line, which carries other missense mutations or a stop codon mutation. In human patients, some correlation between FKRP mutation and disease phenotype has been found.[18] For example, the L276I (C826A) mutation causes the mild phenotype LGMD2I, but the P448L mutation causes severe congenital muscular dystrophy. The homozygous P448L^{KI} mouse model recreates the severe clinical phenotype.[21] The compound heterozygous mutation between the common L276I and either other missense mutations or a nonsense mutation causes the intermediate Duchenne-like severity; the compound heterozygous FKRP mutation between a nonsense mutation and a missense mutation or one that carries two missense mutations triggers the onset of the severe phenotype, with or without eye and brain involvement.[18]

In addition to the muscle pathology, cardiomyopathy is often found in LGMD2I patients.[39,40] We also observed cardiac fibrosis and cell infiltration in the FKRP *L276I*^{KI} model. However, echocardiography did not detect any significant difference between the homozygotes and their heterozygous carrier control mice. No differences were found in the gene therapy treated mice either, despite overexpression of the *FKRP* gene in the heart. This phenomenon brought to mind previous findings in the *mdx* mice, which also displayed cardiac fibrosis and cardiomyopathy, but echocardiography variations were insignificant until mice reached an older age.[36] Nonetheless, the contractile function deficit of the *mdx* heart can be exacerbated becoming readily detectable when the cardiac stress test was induced by dobutamine treatment.[36] Similarly, the FKRP *L276I*^{KI} mice also displayed significant cardiac function deficits by dobutamine-induced cardiac stress, as shown by the echocardiography (**Figure 4**). Gene therapy treated mice showed functional improvement compared to the heterozygous controls, suggesting efficient function recovery by FKRP overexpression without evidence of cardiac toxicity.

We did not see systemic toxicity associated with either AAV9-CB-FKRP vector that contains a ubiquitous promoter or the AAV9-Syn100-FKRP vector that contains a striated muscle-specific promoter. Furthermore, no additional functional improvements were observed between the syn100 promoter and the CB promoter. Although the *FKRP* gene is expressed in many nonmuscle tissues,[9] the liver and kidney functions were found to be normal in the mutant mice, which was verified by their normal serum ALT and BUN levels (**Supplementary Figure S3**). Understandably, a striated muscle-specific promoter is preferable for the purpose of systemic gene therapy. However, nonspecific expression of FKRP in the liver and the kidney was not found to cause any harm and could even provide beneficial effect to those tissues. Previously, overexpression of the LARGE gene induced hyperglycosylation of α-DG in skeletal and cardiac muscle causing toxicity.[9] LARGE has a similar function to FKRP, since it phosphorylates the O-linked mannose on α-DG. Nevertheless, we did not observe similar hyperglycosylation effects associated with the overexpression of FKRP in our *L276I*^{KI} model, suggesting *FKRP* gene therapy has a large safety margin and is an excellent approach for treating FKRP deficiency and other related dystroglycanopathties.

MATERIALS AND METHODS

Generation of the FKRP animal model and genotyping. The method used to create the knock-in mice was carefully described previously.[21] Briefly, the FKRP KI mice were generated by the UNC core facility. The targeting vector was engineered with a c.826 C>A point mutation resulting in an amino acid change from leucine to isoleucine at position 276. The neomycin resistant (Neo^r) cassette was placed into intron 2 about 140 bp upstream from the coding exon 3. The PCR primers for genotyping the

heterozygous and homozygous mice were listed as follows: FKRP-WT-F: TTC TTG CCT CGG ATT GTG TAT G; FKRP-WT-R: TCA CTC TCC AAG GGC CTA CAG C; Neo-F-FKRP: AAC AAG ATG GAT TGC ACG CAG G; Neo-R-FKRP: TGG TCG AAT GGG CAG GTA G.

Plasmid construction and AAV vector production. The codon optimized human FKRP cDNA with myc tag fragments was synthesized from a commercial company (GeneArt, Grand Island, NY). By digesting with restriction enzymes, *Not*I and *Sal*I, the cDNA fragments were cohesively ligated to the AAV backbone vector pXX-UF1, containing a CB promoter.[41,42] The final construct was named pXX-UF1-CB-FKRP-myc. Syn100 was based upon a synthetic muscle promoter (SP c5-12), which was screened from randomly assembled myogenic element libraries.[35] To increase tissue specificity and promoter strength, the downstream +100 bp sequence (cga gct acc cgg agg agc ggg agg cgt ctc tgc cag cgg tcc gac gcg cag tca gca cca ggt agg tgg gca ccg cgc cgt gcc gtg ccg tgc cgt gccg) of chicken skeletal α-actin promoter was added to the end of SP c5-12, and the new promoter was designated as syn100. To construct AAV vector plasmid containing syn100 promoter (pXX-UF1-syn100-FKRP), the PCR product of syn100 promoter (flanked by *Kpn*I and *Hpa*I) was cloned into the *Kpn*I and *Hpa*I sites of pXX-UF1-CB-FKRP in order to replace the CB promoter.

AAV vectors were produced by triple transfection method[43] and the virus was purified by polyethylene glycol (PEG) precipitation followed by CsCl centrifugation.[44] The virus titer was determined by both dot-blot and real-time PCR methods.[45,46] The concentration of the viral vectors was in the range of 2×10^{12} to 5×10^{12} vgs per milliliter (vg/ml).

Collagen staining and quantification. Two methods, Masson's Trichrome staining and Sirius red/Fast green staining, were used for collagen display. The Masson trichrome stain kit was commercially available (IMEB, San Marcos, CA; cat# K7228), and the instructor's protocol was strictly followed. For Sirius red/Fast green staining, first, 10-μm cryo-section tissues were fixed with ice-cold acetone for 5 minutes. Following three repeated washings with tap water, the slides were then stained in 0.1% fast green for 15–20 minutes, and next in 0.1% Sirius red for 4 minutes. The stained slides were subjected to either dehydration and mounting for examination and pictures or elution for collagen quantification.

The collagen and noncollagen proteins were eluted from the stained slides using a dye extraction solution (a 1:1 mixture of 0.1 N NaOH and methanol) with gentle pipetting. Then, samples were quantified by protein measurement at wavelengths 540 and 605 nm. Formulas to calculate the collagen and total noncollagen protein are as follows: collagen (μg/section) = $(A_{540\ nm}-(A_{605\ nm}\times0.291))/37.8\times1{,}000$, where $A_{540\ nm}$ and $A_{605\ nm}$ are the absorbance at 540 and 605 nm, respectively; noncollagen protein (μg/section) = $A_{605\ nm}/2.04\times1{,}000$. The ratio of collagen to noncollagen protein was presented in the **Figures 1d** and **3d**.

Mice and vector administration. All protocols involving animal experiments were approved by the University of North Carolina Animal Care and Use Committee. C57BL/6 mice were purchased from The Jackson Laboratory (Bar Harbor, ME). The L276I FKRP knock-in mice were generated and adapted from the UNC core facility. For systemic studies, the AAV serotype 9 FKRP vectors were delivered into the neonates (3–5 days old, 10 mice/group) of B6 background L276I FKRP KI mice by intraperitoneal injection (total 1×10^{11} vg/mouse).[47] For adult injection, the vectors (6×10^{13} vg/kg) were delivered into the 9-month-old male mice through tail vein injection.

Immunofluorescent staining, western blot, and histology examination. The immunofluorescent staining was performed according to the previously published protocol.[31,48] Since the anti-α-DG antibody (kindly provided by Dr Kevin P Campbell) was a monoclonal antibody (1:50 dilution), the mouse on mouse blocking reagent (VECTOR MKB-2213) was applied to the 8-μm cryo-section tissues right after the regular blocking procedure (with 10% horse serum) to prevent high background staining. For FKRP staining, the cryo-thin section tissues were fixed in 4% paraformaldehyde for 15 minutes. The rabbit polyclonal anti-FKRP antibody (raised against the last 15 residues of mouse FKRP sequence, NPE YPN PAL LSL TGG, kindly provide by Dr Lu's laboratory) was used at 1:400 dilution. The rabbit polyclonal anti-myc antibody was from Abcam (Cambridge, MA; Catalog # ab9106). It was applied at 1:200 dilution. Photographs were taken with a Nikon Eclipse TE300 microscope, using a SPOT RT SLIDER digital camera (Diagnostic Instrument, Life Technologies, Grand Island, NY).

The protocol of western blot against α-DG has been described previously.[21] Briefly, the total proteins were dissolved in TX-100 buffer (1% Triton X-100, 50 mmol/l Tris, PH 8.0, 150 mmol/l NaCl, 0.1% sodium dodecyl sulfate (SDS)) supplemented with protease inhibitor cocktail (Sigma-Aldrich, St. Louis, MO). For the western blot against FKRP, total proteins were extracted from tissues of interest using lysis buffer containing 4% SDS, 125 mmol/l Tris PH 8.8, 4% glycerol, 100 mmol/l DTT (dithiothreitol), 0.01% BPB (bromophenol blue), and protease inhibitor cocktail. Protein concentration was determined by BCA protein assay kit (Pierce, Rockford, IL; Cat # 23227). Proteins (15 μg for each sample) were separated by 8–10% SDS–polyacrylamide gel electrophoresis (PAGE) and transferred to polyvinylidene fluoride membranes and probed with α-DG antibody (1:1,000), or FKRP antibody (1:4,000), and developed with horseradish peroxidase–enhanced chemiluminescence.

H&E staining was performed for histology examination. In order to calculate the centrally located nuclei, three images (objective lens ×10) were taken from each muscle. All the fibers (roughly 1,000 fibers from each muscle) were counted from printed images.

Serum creatine kinase enzyme assay. Serum CK enzyme activities were measured with a creatine kinase reagent kit (Pointe Scientific, Canton, MI; catalog # C7512-120). The procedure was followed exactly according to the manufacturer's instruction.

In vivo *myofiber plasma membrane integrity test.* Evans blue dye (10 mg/ml phosphate-buffered saline) was injected into the tail vein of heterozygous and homozygous FKRP *L276I* mice at the dose of 0.1 mg/g of body weight.[25] After dye injection, mice were subjected to treadmill running (at a 15° downward angle at a rate of 15 m/minute) for 20 minutes. At 16 hours after Evans blue injection, the mice were sacrificed and muscles were collected and cryo-sectioned. Evans blue dye-positive myofibers were observed under the fluorescent microscope with rhodamine filters.

Muscle function analysis. The fore limb grip force was performed using the digital force gauge (Chatillon Ametek, Largo, FL) as previously described.[49] The treadmill tests were described in our previous study.[28] Briefly, both treated and nontreated mice were placed on a motorized treadmill (Harvard Apparatus, Holliston, MA; model 7054) to run at a 15° downward angle at a rate of 15 m/minute. The test was stopped after the animal spent 5 seconds sitting on the shock grid without attempting to re-enter the treadmill.

The *in vitro* contraction functional measurement was performed according to the previously published protocol, except for using a different model of transducer (Model 300B, dual mode; Aurora Scientific, Aurora, Ontario, Canada).[48] Briefly, the TA muscle was isolated by removing the overlying bicep femoris and gently opening the fascia of the anterior compartment. The distal portion of the TA tendon was secured with a 4-0 silk suture, and the entire TA was removed with its tibial origin intact. The TA tibial origin was fixed by securing the head of the tibia with a vascular clamp mounted in series to a micropositioner near the base of the tissue chamber. The tissue chamber was constantly perfused with mammalian Ringer's solution aerated with 95% O_2–5% CO_2 and maintained at 25 °C. Care was taken to position the tibia in a vertical orientation so that the TA fibers were in vertical alignment. The muscle was stimulated by using the single pulse program (Stimulator model No 701A and A/D interface). Then, the muscle length was adjusted, and the muscle was restimulated with the single pulse program in order to find the optimal wave length and

maximal twitch force. Two minutes of resting time were given between stimulations. Tetanic force measurement and eccentric contraction testing were performed using fixed protocols specifically for tetanic stimulation and stretch stimulation. For tetanic force measurement, different stimulating frequencies (50, 75, 100, and 125 Hz) were utilized, and the maximal tetanic force (P_o) was obtained. For eccentric contraction test (10 cycles), the specific value of individual muscle length was entered into the program to guarantee an accurate lengthening stretch. A 2-minute resting period was given between stimulation cycles. Following these measurements, the stimulated muscle was weighed on an analytic balance (Mettler Toledo, Columbia, MD; D521512), after the tendon and bone attachments were removed and the muscle was blotted dry. The specific tetanic forces (N/cm^2) were calculated using the following formula:

$$\frac{maximal\,tenanic\,force\,(g)}{\left(\frac{muscle\,weight\,(g)}{muscle\,length\,(cm)}\right)\times\left(\frac{cm^3}{1.056g}\right)}\times\frac{kg}{1{,}000g}\times\frac{9.8N}{kg}=\frac{N}{cm^2}$$

Echocardiography. The echocardiography (Echo) analysis was described previously.[38] Dobutamine was purchased from Sigma-Aldrich (catalog # D0676 -10MG). Experimental mice were sedated with 2.5% avertin (150 ìl/10 g body weight). The freshly diluted dobutamine (2.25 µg/g body weight) was immediately injected into the mice via intraperitoneal delivery. The heart rate was increased by roughly 100 beats per minute after dobutamine stimulation. The second Echo was performed 2 minutes after dobutamine stimulation once the heart rate remained stable. The three M-mode graphs were saved for analysis from each Echo. There were three to eight mice involved in each group.

Statistical analysis. Values are expressed as means ± SD. Welch's *t*-test was applied when comparing two groups. When comparing three groups, one-way analysis of variance plus Dunnett post-test was applied using Graph Pad Prism software (GraphPad Software, La Jolla, CA). A $P < 0.05$ was considered statistically significant.

SUPPLEMENTARY MATERIAL

Figure S1. The muscle pathology of homozygous FKRP *L276I*^{KI} mice was focal.

Figure S2. The muscle forces generated by homozygous FKRP *L276I*^{KI} mice were weaker.

Figure S3. Serum ALT and BUN levels.

Figure S4. Expression of FKRP confirmed by anti-myc staining.

ACKNOWLEDGMENTS

We sincerely thank Kevin P Campbell (University of Iowa) for providing the IIH6 antibody. This project was supported by NIH grant R01 NS082536 to X.X. and the McColl-Lockwood Foundation Endowment to Q.L. No conflict of interest to disclose.

REFERENCES

1. Emery, AE (2002). The muscular dystrophies. *Lancet* **359**: 687–695.
2. Michele, DE, Barresi, R, Kanagawa, M, Saito, F, Cohn, RD, Satz, JS *et al.* (2002). Post-translational disruption of dystroglycan-ligand interactions in congenital muscular dystrophies. *Nature* **418**: 417–422.
3. Godfrey, C, Clement, E, Mein, R, Brockington, M, Smith, J, Talim, B *et al.* (2007). Refining genotype phenotype correlations in muscular dystrophies with defective glycosylation of dystroglycan. *Brain* **130**(Pt 10): 2725–2735.
4. Mercuri, E, Brockington, M, Straub, V, Quijano-Roy, S, Yuva, Y, Herrmann, R *et al.* (2003). Phenotypic spectrum associated with mutations in the fukutin-related protein gene. *Ann Neurol* **53**: 537–542.
5. Kuga, A, Kanagawa, M, Sudo, A, Chan, YM, Tajiri, M, Manya, H *et al.* (2012). Absence of post-phosphoryl modification in dystroglycanopathy mouse models and wild-type tissues expressing non-laminin binding form of α-dystroglycan. *J Biol Chem* **287**: 9560–9567.
6. Bowe, MA, Deyst, KA, Leszyk, JD and Fallon, JR (1994). Identification and purification of an agrin receptor from Torpedo postsynaptic membranes: a heteromeric complex related to the dystroglycans. *Neuron* **12**: 1173–1180.
7. Sugita, S, Saito, F, Tang, J, Satz, J, Campbell, K and Südhof, TC (2001). A stoichiometric complex of neurexins and dystroglycan in brain. *J Cell Biol* **154**: 435–445.
8. Barresi, R and Campbell, KP (2006). Dystroglycan: from biosynthesis to pathogenesis of human disease. *J Cell Sci* **119**(Pt 2): 199–207.
9. Brockington, M, Torelli, S, Sharp, PS, Liu, K, Cirak, S, Brown, SC *et al.* (2010). Transgenic overexpression of LARGE induces α-dystroglycan hyperglycosylation in skeletal and cardiac muscle. *PLoS One* **5**: e14434.
10. Longman, C, Brockington, M, Torelli, S, Jimenez-Mallebrera, C, Kennedy, C, Khalil, N *et al.* (2003). Mutations in the human LARGE gene cause MDC1D, a novel form of congenital muscular dystrophy with severe mental retardation and abnormal glycosylation of alpha-dystroglycan. *Hum Mol Genet* **12**: 2853–2861.
11. van Reeuwijk, J, Janssen, M, van den Elzen, C, Beltran-Valero de Bernabé, D, Sabatelli, P, Merlini, L *et al.* (2005). POMT2 mutations cause alpha-dystroglycan hypoglycosylation and Walker-Warburg syndrome. *J Med Genet* **42**: 907–912.
12. Beltran-Valero de Bernabe, D, Currier, S and Brunner, HG. (2002). Mutations in the O-mannosyltransferase gene POMT1 give rise to the severe neuronal migration disorder Walker-Warburg syndrome. *Am J Human Genet* **71**: 1033–1043.
13. Yoshida, A, Kobayashi, K, Manya, H, Taniguchi, K, Kano, H, Mizuno, M *et al.* (2001). Muscular dystrophy and neuronal migration disorder caused by mutations in a glycosyltransferase, POMGnT1. *Dev Cell* **1**: 717–724.
14. Kobayashi, K, Nakahori, Y, Miyake, M, Matsumura, K, Kondo-Iida, E, Nomura, Y *et al.* (1998). An ancient retrotransposal insertion causes Fukuyama-type congenital muscular dystrophy. *Nature* **394**: 388–392.
15. Brockington, M, Yuva, Y, Prandini, P, Brown, SC, Torelli, S, Benson, MA *et al.* (2001). Mutations in the fukutin-related protein gene (FKRP) identify limb girdle muscular dystrophy 2I as a milder allelic variant of congenital muscular dystrophy MDC1C. *Hum Mol Genet* **10**: 2851–2859.
16. Manya, H, Chiba, A, Yoshida, A, Wang, X, Chiba, Y, Jigami, Y *et al.* (2004). Demonstration of mammalian protein O-mannosyltransferase activity: coexpression of POMT1 and POMT2 required for enzymatic activity. *Proc Natl Acad Sci USA* **101**: 500–505.
17. Yoshida-Moriguchi, T, Yu, L, Stalnaker, SH, Davis, S, Kunz, S, Madson, M *et al.* (2010). O-mannosyl phosphorylation of alpha-dystroglycan is required for laminin binding. *Science* **327**: 88–92.
18. Brown, SC, Torelli, S, Brockington, M, Yuva, Y, Jimenez, C, Feng, L *et al.* (2004). Abnormalities in alpha-dystroglycan expression in MDC1C and LGMD2I muscular dystrophies. *Am J Pathol* **164**: 727–737.
19. Hong, D, Zhang, W, Wang, W, Wang, Z and Yuan, Y (2011). Asian patients with limb girdle muscular dystrophy 2I (LGMD2I). *J Clin Neurosci* **18**: 494–499.
20. Beltran-Valero de Bernabe, D, Voit, T, Longman, C, Steinbrecher, A, Straub, V, Yuva, Y *et al.* (2004). Mutations in the FKRP gene can cause muscle-eye-brain disease and Walker-Warburg syndrome. *J Med Genet* **41**: e61.
21. Chan, YM, Keramaris-Vrantsis, E, Lidov, HG, Norton, JH, Zinchenko, N, Gruber, HE *et al.* (2010). Fukutin-related protein is essential for mouse muscle, brain and eye development and mutation recapitulates the wide clinical spectrums of dystroglycanopathies. *Hum Mol Genet* **19**: 3995–4006.
22. Wang, CH, Chan, YM, Tang, RH, Xiao, B, Lu, P, Keramaris-Vrantsis, E *et al.* (2011). Post-Natal knockdown of fukutin-related protein expression in muscle by long-termRNA interference induces dystrophic pathology [corrected]. *Am J Pathol* **178**: 261–272.
23. Xu, L, Lu, PJ, Wang, CH, Keramaris, E, Qiao, C, Xiao, B *et al.* (2013). Adeno-associated virus 9 mediated FKRP gene therapy restores functional glycosylation of α-dystroglycan and improves muscle functions. *Mol Ther* **21**: 1832–1840.
24. Xiao, X, Li, J and Samulski, RJ (1996). Efficient long-term gene transfer into muscle tissue of immunocompetent mice by adeno-associated virus vector. *J Virol* **70**: 8098–8108.
25. Wang, B, Li, J and Xiao, X (2000). Adeno-associated virus vector carrying human minidystrophin genes effectively ameliorates muscular dystrophy in mdx mouse model. *Proc Natl Acad Sci USA* **97**: 13714–13719.
26. Harper, SQ, Hauser, MA, DelloRusso, C, Duan, D, Crawford, RW, Phelps, SF *et al.* (2002). Modular flexibility of dystrophin: implications for gene therapy of Duchenne muscular dystrophy. *Nat Med* **8**: 253–261.
27. Kornegay, JN, Li, J, Bogan, JR, Bogan, DJ, Chen, C, Zheng, H *et al.* (2010). Widespread muscle expression of an AAV9 human mini-dystrophin vector after intravenous injection in neonatal dystrophin-deficient dogs. *Mol Ther* **18**: 1501–1508.
28. Qiao, C, Li, J, Zhu, T, Draviam, R, Watkins, S, Ye, X *et al.* (2005). Amelioration of laminin-alpha2-deficient congenital muscular dystrophy by somatic gene transfer of miniagrin. *Proc Natl Acad Sci USA* **102**: 11999–12004.
29. Stedman, HH, Sweeney, HL, Shrager, JB, Maguire, HC, Panettieri, RA, Petrof, B *et al.* (1991). The mdx mouse diaphragm reproduces the degenerative changes of Duchenne muscular dystrophy. *Nature* **352**: 536–539.
30. Mokuno, K, Riku, S, Sugimura, K, Takahashi, A, Kato, K and Osugi, S (1987). Serum creatine kinase isoenzymes in Duchenne muscular dystrophy determined by sensitive enzyme immunoassay methods. *Muscle Nerve* **10**: 459–463.
31. Watchko, J, O'Day, T, Wang, B, Zhou, L, Tang, Y, Li, J *et al.* (2002). Adeno-associated virus vector-mediated minidystrophin gene therapy improves dystrophic muscle contractile function in mdx mice. *Hum Gene Ther* **13**: 1451–1460.
32. Wang, Z, Zhu, T, Qiao, C, Zhou, L, Wang, B, Zhang, J *et al.* (2005). Adeno-associated virus serotype 8 efficiently delivers genes to muscle and heart. *Nat Biotechnol* **23**: 321–328.
33. Sveen, ML, Thune, JJ, Køber, L and Vissing, J (2008). Cardiac involvement in patients with limb-girdle muscular dystrophy type 2 and Becker muscular dystrophy. *Arch Neurol* **65**: 1196–1201.
34. Wang, B, Li, J, Fu, FH, Chen, C, Zhu, X, Zhou, L *et al.* (2008). Construction and analysis of compact muscle-specific promoters for AAV vectors. *Gene Ther* **15**: 1489–1499.
35. Li, X, Eastman, EM, Schwartz, RJ and Draghia-Akli, R (1999). Synthetic muscle promoters: activities exceeding naturally occurring regulatory sequences. *Nat Biotechnol* **17**: 241–245.
36. Wu, B, Moulton, HM, Iversen, PL, Jiang, J, Li, J, Li, J *et al.* (2008). Effective rescue of dystrophin improves cardiac function in dystrophin-deficient mice by a modified morpholino oligomer. *Proc Natl Acad Sci USA* **105**: 14814–14819.
37. Mertes, H, Sawada, SG, Ryan, T, Segar, DS, Kovacs, R, Foltz, J *et al.* (1993). Symptoms, adverse effects, and complications associated with dobutamine stress echocardiography. Experience in 1118 patients. *Circulation* **88**: 15–19.

38. He, B, Tang, RH, Weisleder, N, Xiao, B, Yuan, Z, Cai, C *et al.* (2012). Enhancing muscle membrane repair by gene delivery of MG53 ameliorates muscular dystrophy and heart failure in δ-Sarcoglycan-deficient hamsters. *Mol Ther* **20**: 727–735.
39. Hollingsworth, KG, Willis, TA, Bates, MG, Dixon, BJ, Lochmüller, H, Bushby, K *et al.* (2013). Subepicardial dysfunction leads to global left ventricular systolic impairment in patients with limb girdle muscular dystrophy 2I. *Eur J Heart Fail* **15**: 986–994.
40. Wahbi, K, Meune, C, Hamouda, el H, Stojkovic, T, Laforêt, P, Bécane, HM *et al.* (2008). Cardiac assessment of limb-girdle muscular dystrophy 2I patients: an echography, Holter ECG and magnetic resonance imaging study. *Neuromuscul Disord* **18**: 650–655.
41. Li, J, Dressman, D, Tsao, YP, Sakamoto, A, Hoffman, EP and Xiao, X (1999). rAAV vector-mediated sarcogylcan gene transfer in a hamster model for limb girdle muscular dystrophy. *Gene Ther* **6**: 74–82.
42. Qiao, C, Yuan, Z, Li, J, He, B, Zheng, H, Mayer, C *et al.* (2011). Liver-specific microRNA-122 target sequences incorporated in AAV vectors efficiently inhibits transgene expression in the liver. *Gene Ther* **18**: 403–410.
43. Xiao, X, Li, J and Samulski, RJ (1998). Production of high-titer recombinant adeno-associated virus vectors in the absence of helper adenovirus. *J Virol* **72**: 2224–2232.
44. Ayuso, E, Mingozzi, F, Montane, J, Leon, X, Anguela, XM, Haurigot, V *et al.* (2010). High AAV vector purity results in serotype- and tissue-independent enhancement of transduction efficiency. *Gene Ther* **17**: 503–510.
45. Rohr, UP, Heyd, F, Neukirchen, J, Wulf, MA, Queitsch, I, Kroener-Lux, G *et al.* (2005). Quantitative real-time PCR for titration of infectious recombinant AAV-2 particles. *J Virol Methods* **127**: 40–45.
46. Veldwijk, MR, Topaly, J, Laufs, S, Hengge, UR, Wenz, F, Zeller, WJ *et al.* (2002). Development and optimization of a real-time quantitative PCR-based method for the titration of AAV-2 vector stocks. *Mol Ther* **6**: 272–278.
47. Qiao, C, Li, J, Jiang, J, Zhu, X, Wang, B, Li, J *et al.* (2008). Myostatin propeptide gene delivery by adeno-associated virus serotype 8 vectors enhances muscle growth and ameliorates dystrophic phenotypes in mdx mice. *Hum Gene Ther* **19**: 241–254.
48. Xiao, X, Li, J, Tsao, YP, Dressman, D, Hoffman, EP and Watchko, JF (2000). Full functional rescue of a complete muscle (TA) in dystrophic hamsters by adeno-associated virus vector-directed gene therapy. *J Virol* **74**: 1436–1442.
49. Bojak, A, Hammer, D, Wolf, H and Wagner, R (2002). Muscle specific versus ubiquitous expression of Gag based HIV-1 DNA vaccines: a comparative analysis. *Vaccine* **20**: 1975–1979.